Inorganica Chimica Acta 398 (2013) 117–123

Contents lists available at SciVerse ScienceDirect

Inorganica Chimica Acta

journal homepage: www.elsevier.com/locate/ica

Thiosaccharinate binding to palladium(II) and platinum(II): Synthesis and molecular structures of sulfur-bound complexes [M(κ^1-tsac)$_2$(κ^2-diphosphane)]

Subhi A. Al-Jibori [a,*], Mohamed H.S. Al-Jibori [a], Graeme Hogarth [b,*]

[a] Department of Chemistry, College of Science, University of Tikrit, Tikrit, Iraq
[b] Department of Chemistry, University College London, 20 Gordon Street, London WC1H OAJ, UK

ARTICLE INFO

Article history:
Received 21 September 2012
Received in revised form 6 December 2012
Accepted 7 December 2012
Available online 29 December 2012

Keywords:
Platinum
Palladium
Thiosaccharinate
Diphosphane
X-ray crystallography

ABSTRACT

Palladium(II) and platinum(II) thiosaccharinate complexes [M(κ^1-tsac)$_2$\{κ^2-Ph$_2$P(CH$_2$)$_n$PPh$_2$\}] (M = Pd, Pt; n = 1–4) have been prepared, palladium complexes from reaction of [Pd(tsac)$_2$]·H$_2$O with diphosphanes and platinum complexes from addition of thiosaccharin to [PtCl$_2$\{κ^2-Ph$_2$P(CH$_2$)$_n$PPh$_2$\}] in the presence of triethylamine. All complexes have been fully characterized and the crystal structures of [Pd(κ^1-tsac)$_2$(κ^2-dppp)] (n = 3) and [Pt(κ^1-tsac)$_2$(κ^2-dppm)] (n = 1) have been determined confirming that thiosaccharinate ligands are S-bound. The larger ring complexes (n = 3, 4) are fluxional in solution being attributed to the conformational flexibility of the diphosphane backbones The bis(diphosphane) complexes, [M(κ^1-tsac)$_2$(κ^1-dppm)$_2$] (M = Pd, Pt), have also been prepared upon treatment of [Pd(tsac)$_2$]·H$_2$O with two equivalents of dppm or addition of thiosaccharin to [Pt(κ^2-dppm)$_2$]Cl$_2$ in the presence of triethylamine in which the diphosphanes bind in a monodentate fashion. Both are highly fluxional in solution, changes in the ^{31}P{^{1}H} NMR spectra as a function of temperature being interpreted as the exchange of bound and unbound phosphorus atoms.

1. Introduction

Due to the widespread use of saccharin as an artificial sweetener, the coordination chemistry of this cyclic amide has been widely studied over the past 20 years [1]. Replacement of the carbonyl by a thiocarbonyl gives thiosaccharin and while the two molecules look superficially similar they differ in both their ground state structures and their ligating properties to metal centers. Thus, while saccharin (sacH) exists in a single form (amide), thiosaccharin (tsacH) can adopt two tautomeric forms in solution, namely amide or thiol (Chart 1). Further upon deprotonation the negative charge remains on nitrogen in saccharinate but is primarily located on sulfur in thiosaccharinate (Chart 1) [2,3]. This becomes important for the coordination chemistry of the two amides since the thiosaccharinate (tsac) ligand is expected to bind strongly to *soft* metal centers *via* the exocyclic sulfur atom and consequently the coordination chemistry of thiosaccharinate [4–14] has been shown to be quite different from that of saccharinate.

In our recent work we have focused on the concurrent binding of diphosphane and amide ligands at platinum(II) and palladium(II) centers [15–20]. We have recently found that addition of sodium saccharinate to [MCl$_2$(κ^2-dppf)] [dppf = 1,1′-bis(diphenylphosphino)ferrocene] affords the mono-substituted complexes [MCl(κ^1-sac)(κ^2-dppf)] even when a large excess of sodium saccharinate is used, and saccharinate is N-bound [18]. By way of comparison we have now investigated the addition of thiosaccharinate (tsac) to platinum(II) and palladium(II) diphosphane centers and find that complexes of the type [M(κ^1-tsac)$_2$(κ^2-diphosphane)] readily form, whereby the thiosaccharinate ligands are both S-bound. We report the X-ray crystal structures of two examples of these and variable temperature NMR studies aimed at elucidating fluxionality in solution. While this work was in progress Quinzani and co-workers reported aspects of the palladium chemistry described herein [13].

2. Experimental

2.1. General

NMR spectra were recorded on a Bruker AMX400 spectrometer at University College London and referenced internally to the residual solvent peak (^{1}H) or externally (^{31}P). IR spectra were recorded on a Shimadzu FT8400 spectrometer as either KBr or CsI discs. Conductivity measurements were made on a Philips PW9526 conductivity meter. Metal salts Na$_2$[PdCl$_4$], K$_2$[PtCl$_4$] and diphosphanes were used as supplied. Thiosaccharin [21], *cis*-[PtCl$_2$(dmso)$_2$] [22], [Pt(dppm)$_2$]Cl$_2$ [23] and [Pd(tsac)$_2$]·H$_2$O [12] were prepared according to literature methods.

* Corresponding authors.
E-mail addresses: subhi_aljibori@yahoo.com (S.A. Al-Jibori), g.hogarth@ucl.ac.uk (G. Hogarth).

0020-1693/$ - see front matter © 2013 Elsevier B.V. All rights reserved.
http://dx.doi.org/10.1016/j.ica.2012.12.022

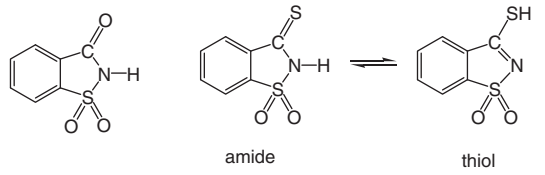

Chart 1.

2.2. Preparation of complexes

2.2.1. $[Pt(tsac)_2]\cdot H_2O$ (**1**)

A solution of thiosaccharin (tsacH) (0.04 g, 0.24 mmol) in methanol (8 cm^3) was added to a solution of $K_2[PtCl_4]$ (0.05 g, 0.12 mmol) in water (3 cm^3). The orange mixture was heated at reflux on a steam bath for 2 h. After cooling to room temperature the brown solid formed was filtered off, washed with water and dried in a vacuum oven to give **1** (0.049 g, 70%). ^{1}H NMR (d^6-dmso): δ 8.50 (d, *J* 7.0 Hz, 2H), 8.86 (d, *J* 6.8 Hz, 2H), 7.76 (m, 4H); IR ν/cm^{-1}; IR(KBr) 3085w, 1419s, 1340vs, 1100vs, 1012s, 804vs, 366m cm^{-1}; Elemental *Anal.* Calc. for $PtS_4N_2O_4C_{14}H_8\cdot H_2O$. Found: C, 27.58 (27.63); H, 1.64 (1.49); N, 4.60 (4.59)%.

2.2.2. $[PtCl_2(\kappa^2\text{-diphosphane})]$

A solution of dppm (0.20 g, 0.52 mmol) in dichloromethane (5 cm^3) was added to *cis*-$[PtCl_2(dmso)_2]$ (0.22 g, 0.52 mmol) suspended in dichloromethane (10 cm^3). The mixture was heated under reflux for 1 h after which it was filtered hot and the filtrate was allowed to evaporate slowly at room temperature. The white solid thus formed was dried under vacuum to give $[PtCl_2(\kappa^2\text{-dppm})]$ (0.17 g, 79%). The complexes $[PtCl_2(\kappa^2\text{-dppe})]$, $[PtCl_2(\kappa^2\text{-dppp})]$ and $[PtCl_2(\kappa^2\text{-dppb})]$ were prepared and isolated employing a similar method.

2.2.3. $[Pd(\kappa^1\text{-tsac})_2(\kappa^2\text{-diphosphane})]$ (**2**–**5**)

For **2**: A solution of dppm (0.036 g, 0.093 mmol) in chloroform (5 cm^3) was added to $[Pd(tsac)_2]\cdot H_2O$ (0.05 g, 0.093 mmol) suspended in chloroform (10 cm^3). The mixture was heated under reflux for 30 min. The brown solution thus formed was filtered and the filtrate was reduced to half volume. Methanol (2 cm^3) was added to this and the mixture was set a side to evaporate slowly at room temperature. The yellow crystalline solid thus formed was filtered off and dried under vacuum (91%). The following complexes were prepared and isolated by a similar method; $[Pd(\kappa^1\text{-tsac})_2(\kappa^2\text{-dppe})]$ (**3**), $[Pd(\kappa^1\text{-tsac})_2(\kappa^2\text{-dppp})]$ (**4**) and $[Pd(\kappa^1\text{-tsac})_2(\kappa^2\text{-dppb})]$ (**5**).

Characterizing data: **2**: yellow solid, 91% yield. ^{1}H NMR: δ 7.80–7.40 (m, 28 H, Ar), 4.23 (t, *J* 12.0, 2H, CH_2); $^{31}P\{^1H\}$ NMR: −40.6 (s) ppm. $^{13}C\{^1H\}$ NMR: 184.5, 138.2, 134.2, 133.4 (t, *J* 6.0 Hz), 132.6, 132.3, 132.2, 129.4 (t, *J* 6.0 Hz), 126.9 (t, *J* 24.1 Hz), 125.1, 120.3, 42.8 (t, *J* 25.6 Hz); IR(KBr) 3058w, 2923w, 1427s, 1318vs, 1159vs, 1000s, 804s, 698m, 367s cm^{-1}; Elemental *Anal.* Calc. for $PdN_2S_4P_2O_4C_{39}H_{30}$. Found: C, 52.80 (52.42); H, 3.38 (3.31); N, 3.16 (3.16)%. **3**: white solid, 82% yield. ^{1}H NMR: δ 7.94–7.42 (m, 28 H, Ar), 2.43 (m, 4H, CH_2); $^{31}P\{^1H\}$ NMR: 61.7 (s) ppm; $^{13}C\{^1H\}$ NMR: 185.6, 137.7, 134.2 (d, *J* 2.0 Hz), 133.7 (d, *J* 10.6 Hz), 132.3, 132.1, 131.3, 129.1 (d, *J* 12.0 Hz), 127.0, 126.7, 124.6, 119.9, 27.5 (dd, *J* 30.2, 13.6 Hz); IR(KBr) 3055w, 2918w, 1423s, 1311vs, 1157vs, 1001s, 808s, 694m, 363s cm^{-1}; Elemental *Anal.* Calc. for $PdN_2S_4P_2O_4C_{40}H_{32}\cdot CH_2Cl_2$. Found: C, 49.93 (50.73); H, 3.45 (3.43); N, 2.84 (2.96)%. **4**: yellow solid, 88% yield. ^{1}H NMR: δ 7.93–7.40 (m, 28 H, Ar), 2.62 (br, 4H, PCH_2), 2.06 (br, 2H, CH_2); $^{31}P\{^1H\}$ NMR: 7.9 (s) ppm; $^{13}C\{^1H\}$ NMR: 185.8, 137.7, 134.3 (d, *J* 1.5 Hz), 133.5 (br), 132.4, 131.4, 128.8, 127.0, 124.7, 120.1, 25.1 (t, *J* 18.1 Hz), 18.4; IR(KBr) 3053w, 2920w, 1422s, 1307vs, 1157vs, 1002s, 806s, 696m, 364s cm^{-1}; Elemental *Anal.* Calc. for $PdN_2S_4P_2O_4C_{41}H_{34}$. Found: C, 53.81 (53.60); H, 3.72 (3.69); N, 3.06 (3.05)%. **5**: yellow–brown solid, 80% yield. ^{1}H NMR: δ 8.10–7.40 (m, 28 H, Ar), 2.60 (br, 4H, CH_2), 2.00 (brs, *J* 20.8 Hz, 2H, PCH_2); $^{31}P\{^1H\}$ NMR: 24.7 (s) ppm; $^{13}C\{^1H\}$ NMR: 185.1, 137.8, 134.1, 133.5 (br), 132.4, 131.4, 131.1 (br), 130.8 (br), 130.4 (br), 128.7 (br), 124.6, 120.1, 26.9 (m), 24.2; IR(KBr) 3057w, 2925w, 1425s, 1309vs, 1157vs, 1000s, 807s, 696m, 365s cm^{-1}; Elemental *Anal.* Calc. for $PdN_2S_4P_2O_4C_{42}H_{36}$. Found: C, 54.29 (53.86); H, 3.88 (3.82); N, 3.02 (3.13)%.

2.2.4. $[Pt(\kappa^1\text{-tsac})_2(\kappa^2\text{-diphosphane})]$ (**6**–**9**)

For **6**: A solution of thiosaccharin (tsacH) (0.06 g, 0.307 mmol) in chloroform (8 cm^3) was added to a solution of $[PtCl_2(\kappa^2\text{-dppm})]$ (0.10 g, 0.154 mmol) in chloroform (10 cm^3). A few drops of triethylamine were added and the resulting mixture was heated under reflex for 1 h. This produced a yellow solution was filtered off and reduced to half volume. Methanol (2 cm^3) was added and the mixture was set a side to evaporate slowly at room temperature. The yellow crystalline solid thus formed was filtered off and dried in a vacuum oven (0.12 g, 91%). Other diphosphane complexes $[Pt(\kappa^1\text{-tsac})_2(\kappa^2\text{-dppe})]$ (**7**), $[Pt(\kappa^1\text{-tsac})_2(\kappa^2\text{-dppp})]$ (**8**) and $[Pt(\kappa^1\text{-tsac})_2(\kappa^2\text{-dppb})]$ (**9**) were prepared and isolated employing a similar method.

Characterizing data: **6**: yellow solid, 91% yield. ^{1}H NMR: δ 7.88 (m, 8H, Ar), 7.63 (m, 2H, Ar), 7.52 (m, 4H, Ar), 7.48 (m, 14H, Ar), 4.46 (t, *J* 10.4, 2H, CH_2); $^{31}P\{^1H\}$ NMR: −50.4 (s, J_{PtP} 2720 Hz) ppm; IR(KBr) 3056w, 2920w, 1425s, 1310s, 1157vs, 996s, 804s, 692m, 371s cm^{-1}; Elemental *Anal.* Calc. for $PtN_2S_4P_2O_4C_{39}H_{30}\cdot 0.5CHCl_3$. Found: C, 45.76 (46.17); H, 2.94 (2.89); N, 2.70 (2.68)%. **7**: yellow solid, 81% yield. ^{1}H NMR: δ 8.0–7.4 (m, 28H, Ar), 2.35 (m, 4H, CH_2); $^{31}P\{^1H\}$ NMR: 45.7 (s, J_{PtP} 3115 Hz) ppm; IR(KBr) 3055w, 2932w, 1427s, 1311s, 1157vs, 999s, 806s, 694s, 375m cm^{-1}; Elemental *Anal.* Calc. for $PtN_2S_4P_2O_4C_{40}H_{32}\cdot CH_2Cl_2$. Found: C, 45.81 (45.07); H, 3.17 (3.24); N, 2.61 (2.51)%. **8**: yellow solid, 82% yield. ^{1}H NMR: δ 7.82 (m, 6H, Ar), 7.67 (d, *J* 7.6 Hz, 2H, Ar), 7.47 (t, *J* 7.6 Hz, 2H, Ar), 7.45–7.25 (m, 18H, Ar), 2.68 (m, 4H, PCH_2), 2.09 (m, 2H, CH_2); $^{31}P\{^1H\}$ NMR: −3.9 (s, J_{PtP} 2970 Hz) ppm; IR(KBr) 3053w, 2923w, 1424s, 1307s, 1157vs, 999s, 805s, 696s, 370m cm^{-1}; Elemental *Anal.* Calc. for $PtN_2S_4P_2O_4C_{41}H_{34}$. Found: C, 49.05 (48.61); H, 3.39 (3.41); N, 2.79 (2.72)%. **9**: yellow–brown solid, 80% yield. ^{1}H NMR: δ 7.90–7.30 (m, 28H, Ar), 2.72 (br, 4H, CH_2), 1.98 (brd, *J* 21.3 Hz, 4H, CH_2); $^{31}P\{^1H\}$ NMR: 11.0 (s, J_{PtP} 3102 Hz) ppm; IR(KBr) 3059w, 2935w, 1429s, 1307s, 1157vs, 995s, 807s, 694s, 374m cm^{-1}; Elemental *Anal.* Calc. for $PtN_2S_4P_2O_4C_{42}H_{36}$. Found: C, 49.56 (48.53); H, 3.54 (3.43); N, 2.75 (2.66)%.

2.2.5. $[Pd(tsac)_2(\kappa^1\text{-dppm})_2]$ (**10**)

A solution of dppm (0.072 g, 0.186 mmol) in chloroform (10 cm^3) was added to $[Pd(tsac)_2]\cdot H_2O$ (0.05 g, 0.093 mmol) suspended in chloroform (10 cm^3). The mixture was heated under reflux for 30 min. The brown solution thus formed was filtered and reduced to half volume. Methanol (2 cm^3) was added and the mixture was set aside to evaporate slowly at room temperature. The pale yellow crystalline solid thus formed was filtered off and dried under vacuum (79%). **10**: pale yellow solid, 79% yield. ^{1}H NMR (d^8-toluene): 293 K δ 8.10–6.40 (m, 48 H, Ar), 3.66 (br, 4H, CH_2); 373 K δ 7.63 (br, 8H), 7.46 (br, 2H), 7.27 (d, *J* 6.7 Hz, 2H), 7.08–6.90 (obscured by solvent), 6.85 (m, 4H), 3.39 (br, 4H); $^{31}P\{^1H\}$ NMR: 243 K 26.4 (s – small), 18.2 (br), −30.8 (br), −40.7 (s – medium) ppm; IR(KBr) 3060w, 2927w, 1431s, 1313vs, 1159vs, 1000s, 809s, 696m, 363s cm^{-1}; Elemental *Anal.* Calc. for $PdN_2S_4P_4O_4C_{64}H_{52}$. Found: C, 60.45 (59.83); H, 4.09 (4.07); N, 2.20 (2.20)%.

*2.2.6. [Pt(κ¹-tsac)₂(κ¹-dppm)₂] (**11**)*

A solution of thiosaccharin (tsacH) (0.084 g, 0.425 mmol) in chloroform (10 cm^3) was added to a solution of $[Pt(\kappa^2\text{-dppm})_2]Cl_2$ (0.22 g, 0.22 mmol) in chloroform (10 cm^3). A few drops of triethylamine were added and the resulting mixture was heated under reflex for 1 h. This produced a yellow solution which was filtered and reduced to half volume. Methanol (2 cm^3) was added and the mixture was set aside to evaporate slowly at room temperature. The pale yellow crystalline solid thus formed was filtered off and dried in a vacuum oven (85%). **11**: pale yellow solid, 85% yield. ^{1}H NMR: δ 7.57 (d, *J* 7.60 Hz, 4H, Ar), 7.50–6.80 (m, 44 H, Ar), 3.46 (br, 4H, CH_2); $^{31}P\{^1H\}$ NMR: 253 K 18.1 (br), −30.4 (br) ppm; 298 K 16.8 (vbr), −28.1 (vbr) ppm; 333 K −23.3 (vbr) ppm; IR(KBr) 3053w, 2932w, 1431s, 1313vs, 1159vs, 994s, 800s, 694s, 378m cm^{-1}; Elemental *Anal.* Calc. for $PtN_2S_4P_4O_4C_{64}H_{52}\cdot 0.5CH_2Cl_2$. Found: C, 55.42 (55.00); H, 3.79 (3.66); N: 2.00 (1.97)%.

2.3. X-ray crystallography

Single crystals were mounted on glass fibers and all geometric and intensity data were taken from these samples using a Bruker SMART APEX CCD diffractometer using graphite-monochromated Mo Kα radiation (λ = 0.71073 Å) at 150 ± 2 K (**4**) and 293 ± 2 K (**6**). Data reduction was carried out with SAINT PLUS and absorption correction applied using the programme SADABS [24]. Structures were solved by direct-methods (for **4**) or Patterson methods (for **6**) and developed using alternating cycles of least-squares refinement and difference-Fourier synthesis. The majority of non-hydrogen atoms were refined with anisotropic displacement parameters. The exception to this was the disordered solvent molecules associated with **6** which were refined anisotropically and hydrogen atoms were excluded. All other hydrogen atoms were placed in calculated positions (riding model). Hydrogen atoms were not placed on solvent of crystallization in structure due to disorder problems with these atoms. Structure solution used SHELXTL PLUS V6.10 program package [25].

2.3.1. Crystallographic data

$[Pd(\kappa^1\text{-tsac})_2(\kappa^2\text{-dppp})]$ (**4**). MeOH: yellow block, size 0.26 × 0.24 × 0.21 mm, triclinic, space group P 1 bar, a = 10.9755(5) Å, b = 11.1596(6) Å, c = 18.1144(9) Å, α = 75.397(1)°, β = 77.504(1)°, γ = 82.693(1)°, V = 2089.9(2) $Å^3$, Z = 2, d_{calc} = 1.499 g/cm^3, μ = 0.767 mm^{-1}, $F(000)$ = 960, final R indices $[F^2 > 2\sigma]$ R_1 = 0.036, wR_2 = 0.101, R indices (all data) R_1 = 0.043, wR_2 = 0.110. $[Pt(\kappa^1\text{-tsac})_2(\kappa^2\text{-dppm})]$ (**6**).0.5$CHCl_3$·2MeOH·H_2O: yellow block, size 0.36 × 0.24 × 0.23 mm, monoclinic, space group C_2/c, a = 29.031(5) Å, b = 20.477(4) Å, c = 15.281(3) Å, β = 105.325(3)°, V = 8761(3) $Å^3$, Z = 8, d_{calc} = 1.691 g/cm^3, μ = 3.610 mm^{-1}, $F(000)$ = 4448, final R indices $[F^2 > 2\sigma]$ R_1 = 0.043, wR_2 = 0.111, R indices (all data) R_1 = 0.059, wR_2 = 0.120.

3. Results and discussion

*3.1. Synthesis of [Pt(tsac)₂]·H₂O (**1**)*

With the aim of preparing complexes of the type $[M(tsac)_2(diphosphane)]$ and given the commercial availability of a range of diphosphanes, then a simple approach seemed be the addition of the latter to $[M(tsac)_2]$ (M = Pt, Pd). Baran and co-workers have previously reported the synthesis of $[Pd(tsac)_2]\cdot H_2O$ formed upon treatment of $Na_2[PdCl_4]$ with thiosaccharin in methanol [12], while very recently Quinzani and co-workers reported formation of $[Pd(tsac)_2]$ upon addition of thiosaccharin to $[Pd(acac)_2]$ in MeCN [13]. Somewhat surprisingly the platinum analogue, $[Pt(tsac)_2]\cdot H_2O$ (**1**), can be prepared in 70% yield as a brown solid upon addition of thiosaccharin to a refluxing methanol solution of $K_2[PtCl_4]$. It has limited solubility in common organic solvents but is readily soluble in dmso giving an orange solution which is indefinitely stable. The structure of these complexes remains unknown. On the basis of spectroscopic data, $[Pd(tsac)_2]\cdot H_2O$ has been proposed to contain a single metal center ligated by a pair of N,S-chelating thiosaccharinate ligands (**A**), however, Quinzani has pointed out that a dimeric structure with four bridging thiosaccharinate (**B**) cannot be ruled out [13] and nor can a polymeric structure (**C**) with bridging thiosaccharinate ligands (Chart 2).

At other metal centers each of these coordination modes have been found for the thiosaccharinate ligand. For example, $[Cd(tsac)_2(py)_3]$ contains one monodentate S-bound and one chelating N,S-thiosaccharinate ligand, the bite-angle in the latter being 57.99(6)° [4], while interestingly closely related $[Cd(tsac)_2(H_2O)]$ contains polymeric chains of four co-ordinate S,O-bridged cadmium centers [11]. It may be that the three complexes discussed here, namely $[Pd(tsac)_2]\cdot H_2O$, $[Pd(tsac)_2]$ and $[Pd(tsac)_2]\cdot H_2O$ (**1**) each have different molecular structures. Quinzani and co-workers have argued for a chelating N,S-ligation in $[Pd(tsac)_2]\cdot H_2O$ on the basis of IR data [13], but the same authors point out that $[Cd(tsac)_2(py)_3]$ and $[Cd(tsac)_2(H_2O)]$ have very similar IR data the main difference being the "splitting" of some peaks in the spectrum of $[Cd(tsac)_2(py)_3]$ resulting from the two different thiosaccharinate coordination modes within the same molecule [4].

For $[Pt(tsac)_2]\cdot H_2O$ the IR spectrum is quite simple, being indicative of the adoption of a high symmetry structure and on this basis we rule out a polymeric structure. The ^{1}H NMR spectrum is also very simple suggesting the existence of a single isomeric form. In related work we have recently crystallographically characterized a related palladium complex containing 2-acetylamino-5-mercapto-1,3,4-thiadiazole (amtaH) ligands [26] which adopts a paddlewheel structure of the formula, $[Pd_2(\mu\text{-amta})_4]$, in which the four amta ligands bridge the metal center *via* an N,S-coordination mode as shown for **B** (Chart 2). We therefore tentatively suggest that $[Pt(tsac)_2]\cdot H_2O$ adopts a related bimetallic structure with the water molecules being either bound to the vacant coordination sites *trans* to the metal–metal vector, or as water of crystallization.

*3.2. Synthesis of thiosaccharinate complexes [M(κ¹-tsac)₂(κ²-diphosphane)] (**2**–**9**)*

Treatment of equimolar amounts of $[Pd(tsac)_2]\cdot H_2O$ with diphosphanes, $Ph_2P(CH_2)_nPPh_2$ (n = 1–4), in chloroform afforded mixed ligand complexes $[Pd(\kappa^1\text{-tsac})_2(\kappa^2\text{-diphosphane})]$ (**2**–**5**) in good yields (80–91%) as air stable yellow solids (Scheme 1). While this manuscript was in progress, Quinzani and co-workers independently reported the synthesis of $[Pd(\kappa^1\text{-tsac})_2(\kappa^2\text{-dppm})]$ (**2**) and $[Pd(\kappa^1\text{-tsac})_2(\kappa^2\text{-dppe})]$ (**3**) along with $[Pd(\kappa^1\text{-tsac})_2(PPh_3)_2]$ using the same synthetic procedure [13].

While the reaction of $[Pd(tsac)_2]\cdot H_2O$ with diphosphanes gave clean products, this method did not work so well with $[Pt(tsac)_2]\cdot H_2O$ (**1**), treatment with diphosphanes leading to a mixture of products which included the desired $[Pt(\kappa^1\text{-tsac})_2(\kappa^2\text{-diphosphane})]$ complexes. The reason for this is not clear but might be related to the stronger platinum–nitrogen versus palladium–nitrogen interactions in $[M(tsac)_2]\cdot H_2O$. In order to alleviate lengthy separation and purification procedures we sought an alternative synthetic route. The diphosphane complexes, $[PtCl_2\{\kappa^2\text{-}Ph_2P(CH_2)_nPPh_2\}]$ (n = 1–4) were readily prepared upon addition of diphosphanes to *cis*-$[PtCl_2(dmso)_2]$ and treatment with thiosaccharin in chloroform in the presence of triethylamine gave the desired $[Pt(\kappa^1\text{-tsac})_2(\kappa^2\text{-diphosphane})]$ (**6**–**9**) in good yields as air-stable pale yellow solids (Scheme 2).

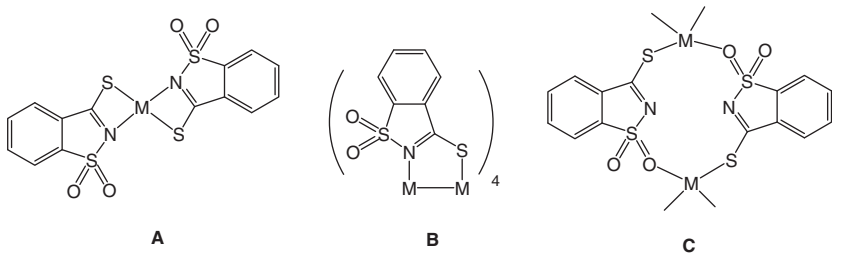

Chart 2.

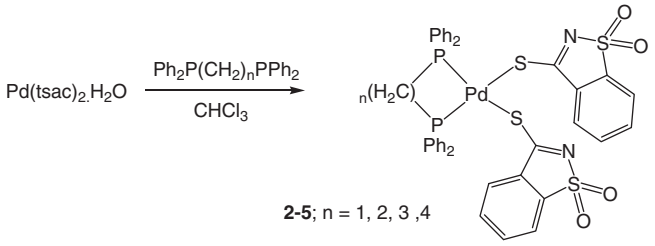

Scheme 1.

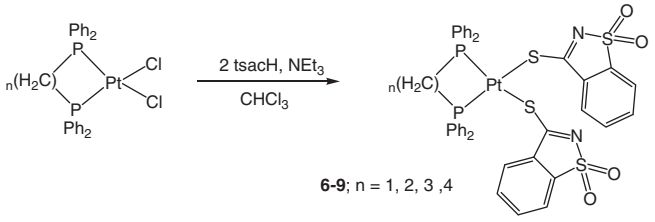

Scheme 2.

Characterization of all thiosaccharinate complexes was relatively straightforward. All palladium complexes showed a singlet resonance in the $^{31}P\{^1H\}$ NMR spectrum, consistent with the formation of bis(thiosaccharinate) complexes. The chemical shift of this signal was found to be highly dependent upon the ring size of the diphosphane. Thus the dppm complex **2** ($n = 1$) appeared at −40.6 ppm, while for **3** ($n = 2$) the singlet appeared at 61.7 ppm. We note that our $^{31}P\{^1H\}$ NMR data are quite different to that reported by Quinzani (**2**: 10.42, **3**: 120.44 ppm) [13]. The reasons for this are not clear. We recorded all our NMR spectra for the diphosphane complexes in $CDCl_3$, while Quinzani recorded all NMR spectra of **3** in d^6-DMSO and also reported that it was an acetonitrile adduct. Thus the differences we see for **3** may relate to the solvent, although such a large change is unexpected. For **2** the difference is even harder to reconcile as both spectra are recorded in $CDCl_3$. In the $^{13}C\{^1H\}$ NMR spectrum all show a low field singlet between 184.59 and 185.79 ppm associated with the carbon atom between the thiol-sulfur and nitrogen atoms. This compares well with a value of 189.69 ppm found in $[Pd(tsac)_2]\cdot H_2O$ [12]. All other signals expected for the thiosaccharinate ligands are also observed in the aromatic region of the spectrum but exact assignment is hampered somewhat by the coincidence of the phenyl carbons of the diphosphane ligands. The diphosphane backbones are easily differentiated as they appear at relatively high field. For **2** (dppm) a simple triplet is observed at 42.76 (J 25.7 Hz), while in **3** the two methylene groups appear as a pseudo doublet of doublets at 27.50 (J 30.2, 13.6 Hz). For both **4** and **5** the phosphorus and non-phosphorus bound methylene groups are easily differentiated, the latter appearing as singlets (**4**: 18.44, **5**: 24.18) and the former as multiplets (**4**: 25.13, t, J 18.1 Hz, **5**: 26.9, m). While all signals in the $^{13}C\{^1H\}$ NMR spectra of **2**–**4** are sharp, in **5** (dppb) there is considerable broadening of some of the signals associated with the phenyl signals of the diphosphane. Thus there are six sharp signals between 140 and 120 ppm associated with the thiosaccharinate ligands, but four very broad signals associated with the diphosphane. This difference is also reflected in the ^1H NMR spectra of the complexes. Thus for **2** and **3** all signals are sharp at room temperature and in line with what is expected (the high field multiplet in **3** is a classic $A_2B_2X_2$ signal). For the dppp complex **4** some signals are sharp but others are broadened, while at room temperature the majority of signals in **5** are broad. We associate the sharp signals in each case with the thiosaccharinate ligands suggesting that these moieties are not participating in the fluxional process. Cooling both samples to 243 K results in further broadening of the signals associated with the diphosphanes, while upon warming to 323 K the spectra sharpen significantly. We have been hampered in fully elucidating the thermodynamic parameters for this process due to the relatively temperature window of $CDCl_3$. Nevertheless it seems apparent that it is associated with a simple flexing of the methylene backbones of the dppp and dppb ligands respectively.

NMR data for the platinum complexes **6**–**9** are broadly similar to the analogous palladium complexes, being somewhat more complicated due to coupling to platinum. Thus the room temperature $^{31}P\{^1H\}$ NMR spectrum in each case shows a singlet with platinum satellites, J_{PtP} coupling constants varying between 2720 and 3115 Hz. As seen with the palladium chemistry, chemical shifts are highly dependent upon ring size. Thus the dppm complex **6** is seen at −50.4 ppm while addition of another methylene group shifts the signal to lower field by near 100 ppm, the dppe complex **7** resonating at 45.7 ppm. The ^1H NMR spectra are also similar to the palladium complexes. Most notably the room temperature spectrum of **9** (dppb) displays a series of sharp resonances associated with the thiosaccharinate ligands but broad resonances for the diphosphane. At higher field, two broad, but well-defined, resonances at δ 2.73 and 1.98 are seen for the methylene protons, the latter being a doublet (J_{PH} 21.3 Hz) attributed to the phosphorus-bound methylene groups. Upon cooling to 223 K, the aromatic resonances sharpen significantly and now four broad resonances are seen for the methylene backbone; again indicative of diphosphane fluxionality. The $^{31}P\{^1H\}$ NMR spectrum also broadens considerably at this temperature but J_{PtP} remains approximately the same (3102 Hz at 313 K, 3079 Hz at 233 K). We did not record the $^{13}C\{^1H\}$ NMR spectra for the platinum complexes.

IR spectra have been widely used to characterize thiosaccharinate complexes [3–14]. For all complexes **2**–**9** the most important bands related to vibrations of the five-membered ring of the thiosaccharinate anions are located between 1500 and 400 cm^{-1}. In particular the presence of ν(CN) (1416–1431 cm^{-1}), ν(CS) (994–1003 cm^{-1}) and ν(NS) (800–822 cm^{-1}) vibrations clearly reflect the coordination of the ligand through its thiocarboxylic sulfur atom. Thus the ν(CS) stretching frequency has shifted from 1037 cm^{-1} in free thiosaccharin to 995–1002 cm^{-1} in the

complexes, reflecting the weakening of the carbon–sulfur bond [2]. The stretching vibration of the SO_2 group produces intense IR bands at 1307–1317 cm^{-1} and 1159 cm^{-1} corresponding to $\nu(SO_2)_{asy}$ and $\nu(SO_2)_{sy}$ respectively. These bands are seen at lower wavenumbers than in thiosaccharin (1373 and 1153 cm^{-1}). Further evidence for the S-bonded thiosaccharinate anion comes from the far IR, a medium to strong band at 355–378 cm^{-1} being assigned to ν(M–S). The coordinated diphosphanes are evident from the appearance of ν(CH) at 2918–2935 cm^{-1} and ν(M–P) at 692–698 cm^{-1}.

3.3. Solid-state structures of [Pd(κ^1-tsac)$_2$(κ^2-dppp)] (**4**) and [Pt(κ^1-tsac)$_2$(κ^2-dppm)] (**6**)

In order to confirm the thiosaccharinate binding mode in these complexes we carried out the X-ray crystal structures of two representative examples, namely [Pd(κ^1-tsac)$_2$(κ^2-dppp)] (**4**) and [Pt(κ^1-tsac)$_2$(κ^2-dppm)] (**6**), the results of which are summarized in Figs. 1 and 2 and Table 1. Fortuitously, Quinzani and co-workers characterized two different palladium complexes, namely [Pd(κ^1-tsac)$_2$(κ^2-dppm)] (**2**) (two molecules in asymmetric unit) and [Pd(κ^1-tsac)$_2$(κ^2-dppe)] (**3**) [13], thus allowing us to make some simple comparisons between changes in the metal and diphosphane backbone. In all complexes of this type the S-bonded thiosaccharinate ligands lie *cis* to one another and the coordination geometry at the metal center is approximately square planar. Within the palladium series, the Pd–P (2.238–2.284 Å) and Pd–S (2.367–2.402 Å) distances vary only slightly as a result of the different diphosphane ligands. As expected, more major differences are seen in the P–Pd–P bite-angles which increase upon sequential addition of a methylene unit [**2**: 73.23(4), 72.84; **3**: 84.86(5); **4**: 90.75(2)°] and this has a less pronounced and less systematic effect on the S–Pd–S bond angles [**2**: 90.93(4), 93.15; **3**: 94.71(5); **4**: 87.97(2)°]. For **4**, the flexible dppp ligand results in the opening of the P–Pd–P angle and concomitant closing of the of the S–Pd–S angle. All three complexes show the same general feature of thiosaccharinate ligands being orientated relatively up and down (*anti*) with respect to the PdS_2P_2 plane, presumably in order to reduce adverse steric interactions and this is effected by the relatively acute Pd–S–C angles subtended at the thiolate sulfur [**4**: Pd(1)–S(1)–C(1) 99.11(9), Pd(1)–S(2)–C(2) 101.26(9)°] being similar to those for **2** [96.8(1)–100.0(1)°] and **3** [97.0(2) and 97.5(2)°]. Bond lengths and angles within the thiosaccharinate ligands do not vary significantly upon changing the diphosphane and are fully consistent with the resonance structures shown in Schemes 1 and 2.

Closer inspection of the dppp complex **4** allows us to better understand the likely fluxional process observed in solution by NMR spectroscopy. Thus in the solid-state (Fig. 1) the six-membered PdP_2C_3 ring adopts a chair configuration with the central methylene unit being orientated upwards (as shown). This should allow for a relatively low energy interconversion to a boat form whereby the central unit inverts. This can easily occur within the ligand sphere of the complex and requires no change in orientation of the two thiosaccharinate ligands. The latter are likely to be fixed even in solution since rotation about either the palladium–sulfur or carbon–sulfur bonds is anticipated to have a high activation barrier. The dppb ligand can likewise interconvert between related ring conformations, while dppe and dppm complexes are more rigid as expected.

The solid-state structure of the platinum complex [Pt(κ^1-tsac)$_2$(κ^2-dppm)] (**6**) is generally similar to the related palladium complex **2**. Platinum-phosphorus [2.234(1) and 2.261(1) Å] and platinum–sulfur [2.335(1) and 2.373(1) Å] distances are within the expected ranges and the diphosphane bite-angle of 73.82(5)° is only slightly larger than those found in **2**. However, the diphosphane bite-angle is not relayed to the two thiolate ligands, the S–Pt–S angle of 86.21(4)° being smaller than any of the related parameters seen at palladium. The main difference between **6** and the palladium structures is seen in the relative orientations of the two thiosaccharinate ligands. Thus, while all three palladium complexes are characterized by an up-down (*anti*) relative arrangement, with both ring systems being placed approximately perpendicular to the PdS_2P_2 plane, in **6** one ring (containing S(2)) lies in this position (angle between planes 74.0°), while the second lies approximately in the PtS_2P_2 plane (angle between planes 5.7°). This also leads to quite different bond angles at sulfur varying from 112.7(2)° in the parallel ring to a more normal 103.1(2)° in that lying perpendicular to the plane.

3.4. Synthesis of thiosaccharinate complexes [M(κ^1-tsac)$_2$(κ^1-dppm)$_2$] (**10**–**11**)

Treatment of [Pd(tsac)$_2$]·H_2O with two equivalents of dppm gave the bis(diphosphane) complex [Pd(κ^1-tsac)$_2$(κ^1-dppm)$_2$] (**10**), while the analogous platinum complex, [Pt(κ^1-tsac)$_2$(κ^1-dppm)$_2$] (**11**), was prepared upon treatment of [Pt(dppm)$_2$]Cl_2

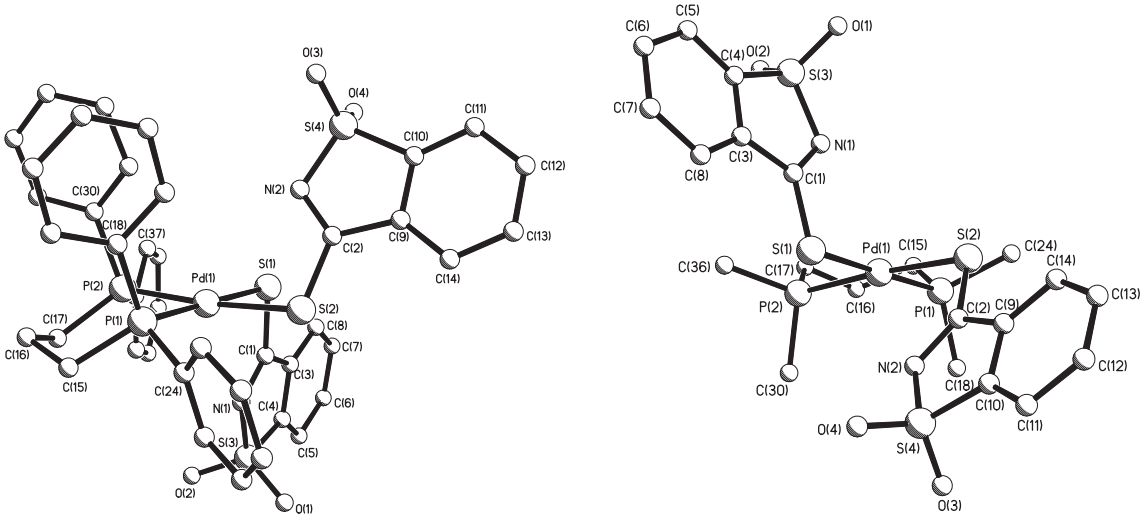

Fig. 1. Two views of the molecular structure of [Pd(κ^1-tsac)$_2$(κ^2-dppp)] (**4**) with selected bond lengths (Å) and angles (°); Pd(1)–P(1) 2.2827(7), Pd(1)–P(2) 2.2844(7), Pd(1)–S(1) 2.3673(6), Pd(1)–S(2) 2.3742(6), S(1)–C(1) 1.703(3), S(2)–C(2) 1.697(3), S(3)–O(1) 1.436(2), S(3)–O(2) 1.440(2), S(3)–N(1) 1.663(2), S(3)–C(4) 1.768(3), S(4)–O(4) 1.443(2), S(4)–O(3) 1.443(2), S(4)–N(2) 1.643(2), S(4)–C(10) 1.767(3), P(1)–Pd(1)–P(2) 90.75(2), S(1)–Pd(1)–S(2) 87.97(2), P(1)–Pd(1)–S(1) 178.81(2), P(2)–Pd(1)–S(2) 174.85(2), Pd(1)–S(1)–C(1) 99.11(9), Pd(1)–S(2)–C(2) 101.36(9).

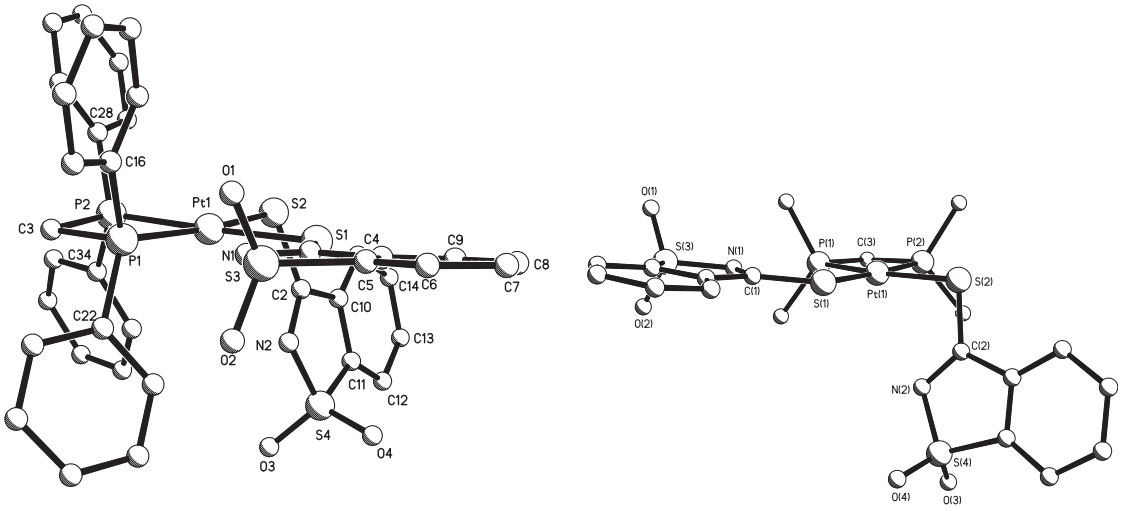

Fig. 2. Two views of the molecular structure of [Pt(κ^1-tsac)$_2$(κ^2-dppm)] (**6**) with selected bond lengths (Å) and angles (°); Pt(1)–P(2) 2.2438(13), Pt(1)–P(1) 2.2613(13), Pt(1)–S(1) 2.3353(13), Pt(1)–S(2) 2.3728(12), S(1)–C(1) 1.698(5), S(2)–C(2) 1.714(5), S(3)–O(1) 1.424(4), S(3)–O(2) 1.434(4), S(3)–N(1) 1.653(4), S(3)–C(5) 1.758(5), S(4)–O(3) 1.430(4), S(4)–O(4) 1.433(4), S(4)–N(2) 1.645(4), S(4)–C(11) 1.765(5), P(1)–Pt(1)–P(2) 73.82(5), S(1)–Pt(1)–S(2) 86.21(4), P(1)–Pt(1)–S(2) 168.04(5), P(2)–Pt(1)–S(1) 177.95(5), Pt(1)–S(1)–C(1) 112.7(2), Pt(1)–S(2)–C(2) 103.1(2).

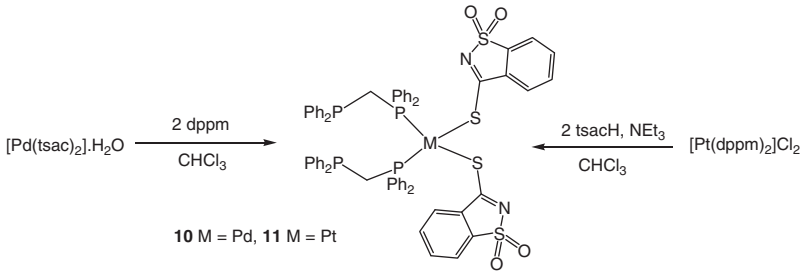

Scheme 3.

with thiosaccharin in the presence of triethylamine (Scheme 3). Both are air-stable lemon yellow solids with relatively poor solubility in common organic solvents. Quinzani has previously reported the preparation of **10** [13].

Characterization as the bis(diphosphane) complexes was made primarily on the basis of elemental analysis data. NMR data for both **10** and **11** are complex and highly temperature dependent. Quinzani and co-workers do not give NMR data for **10** in the experimental section of his paper but say that "$^{31}P\{^1H\}$ NMR spectra show two signals centered at 34 and 15 ppm" [13]. For **10** we cannot see any significant resonances in the $^{31}P\{^1H\}$ NMR spectrum at room temperature. At 243 K two very broad resonances are seen at 18.12 and −30.79 ppm together with a sharp singlet at −40.74 ppm. The two broad resonances are in an approximate 1:1 ratio and are assigned to bound and unbound phosphorus atoms respectively, while the sharp high field signal (ca. 0.5%) is attributed to [Pd(κ^1-tsac)$_2$(dppm)] (**2**). We do not observe a signal at ca. −22 ppm which we might expect for free dppm. ^1H NMR spectra of **10** are difficult to interpret at all temperatures. At 243 K a number of very broad resonances are observed between δ 8.0 – 6.8 and between δ 3.9 – 3.0 there is another broad feature with some fine structure. Upon warming changes occur to both regions but each remains broad and difficult to interpret. Some more insight can be gleaned from the platinum complex and we have recorded a series of $^{31}P\{^1H\}$ NMR spectra for [Pt(κ^1-tsac)$_2$(κ^1-dppm)$_2$] (**11**) in both $CDCl_3$ and d^8-toluene (in both solubility is relatively poor) over the range 373 – 253 K. At 253 K in $CDCl_3$ we observe two broad singlets at 18.06 and −30.37 ppm which we attribute to bound and unbound phosphorus atoms respectively. We were unable to identify any platinum satellites for these signals. Upon warming both broaden such that at room temperature we see two broad resonances at 16.85 and −28.07, while at 333 K all signals have collapsed to give a broad resonance at −23.23 ppm. This indicates that bound and unbound phosphorus atoms are interconverting. The ^1H NMR spectrum at 253 K in $CDCl_3$ shows a series of broad resonances in the aromatic region but a single broad resonance at δ 3.48 associated with the two methylene groups. Upon warming the latter signal broadens but does not change significantly even at 373 K (d^8-toluene: δ 3.39). More informative are the changes in the aromatic region. At 373 K (d^8-toluene) three sharp resonances are seen being attributed to the thiosaccharinate ligand (one resonance is hidden) while other resonances associated with the diphosphane appear as broad singlets. Upon cooling, little changes occur to the thiosaccharinate resonances but the phosphane signals broaden considerably. The poor solubility in toluene precludes the accumulation of data at lower temperatures in this solvent but in $CDCl_3$ the aromatic region of the spectrum again continues to broaden down to 253 K.

We attribute these observations to the interconversion of bound and unbound phosphorus atoms within the complex. We believe that the thiosaccharinate ligands remain essentially unchanged throughout and the NMR spectra show that both are always equivalent. Shaw and co-workers have previously prepared and examined by NMR spectroscopy a series of related organyl complexes, [PtR$_2$(κ^1-dppm)$_2$] [27]. These exist as a mixture of isomers (*syn* and *anti*) differing in the relative orientations of the organyl ligands

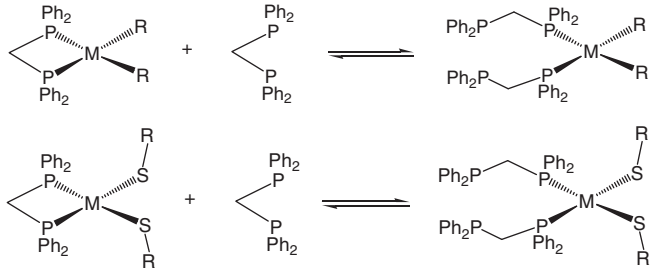

Scheme 4.

with respect to one another which are in equilibrium with [PtR_2(-κ^2-dppm)] and free dppm (Scheme 4).

For **10** and **11**, the bulk of the thiosaccharinate ligands preclude formation of the *syn*-isomer and hence only a single isomer (*anti* up-down arrangement at sulfur). The position of the equilibrium has been found to be highly dependent upon the nature of the organyl ligands. Thus with CH_2R (R = Ph, Bu^t) no bis(diphosphane) complex was observed, while for 1-naphthyl the equilibrium lies strongly over to the bis(diphosphane) complex (K = 78 dm^3 mol^{-1}) [27]. We propose a similar equilibrium for **10** and **11** lying over to the right hand side. For **11** we cannot estimate the equilibrium constant as we do not see [Pt(κ^1-tsac)$_2$(κ^2-dppm)] (**7**) at any temperature. For **10**, we estimate an equilibrium constant of 20 dm^3 mol^{-1} at 243 K {K = Pd(κ^1-tsac)$_2$(κ^1-dppm)$_2$/[Pd(κ^1-tsac)$_2$(κ^2-dppm)]^2 as we could not see free dppm in the spectrum}. There is a large error on this value and it should be treated with caution but it is of a similar magnitude to that found for [$PtPh_2$(κ^1-dppm)$_2$] [27]. Shaw also notes that the time to reach equilibrium varies from minutes to days. For both **10** and **11** equilibrium is established rapidly.

4. Summary

In this contribution we have shown that [MCl_2(κ^2-diphosphane)] complexes react with Na(sac) to afford mono-substituted N-bound complexes [MCl(κ^1-sac)(κ^2-diphosphane)] as the major products and even in the presence of excess Na(sac) the disubstituted complexes are not generated [19]. In contrast, [M(κ^1-tsac)$_2$(κ^2-diphosphane)] are isolated when either [Pd(tsac)$_2$].H_2O is reacted with diphosphanes or when Na(tsac) is added to [$PtCl_2$(κ^2-diphosphane)] and in all the thiosaccharinate ligands are S-bound. In this mode the two thiosaccharinate ligands can adopt a relative *anti*-arrangement resulting in a significant reduction in adverse steric interaction as opposed to unobserved N-bound isomer. With the small bite-angle diphosphane, bis(diphenylphosphino)methane (dppm) [28], the bis(saccharinate) complexes react further to yield [M(κ^1-tsac)$_2$(κ^1-dppm)$_2$] in which the two diphosphanes are monodentate. This is quite different from the behavior observed for other diphosphanes (where no further reaction takes place) and the opening of the chelate ring is probably facilitated by a significant ring-strain in the chelate form. This is not unique to thiosaccharinate and has been observed previously by Shaw and co-workers for related alkyl and aryl complexes [27].

Appendix A. Supplementary material

CCDC 882531 and 882532 contain the supplementary crystallographic data for **4** and **6**. These data can be obtained free of charge from The Cambridge Crystallographic Data Centre *via* www.ccdc.cam.ac.uk/data_request/cif. Supplementary data associated with this article can be found, in the online version, at http://dx.doi.org/10.1016/j.ica.2012.12.022.

References

[1] E.J. Baran, V.T. Yilmaz, Coord. Chem. Rev. 2006 (1980) 250.
[2] M.M. Branda, N.J. Castellani, S.H. Tarulli, O.V. Quinzani, E.J. Baran, R.H. Contreras, Int. J. Quantum. Chem. 89 (2002) 525.
[3] G. Jovanovski, A. Cahil, O. Grupce, L. Pejov, J. Mol. Struct. 784 (2006) 7.
[4] S.H. Tarulli, O.V. Quinzani, E.J. Baran, O.E. Piro, Z. Anorg, Allg. Chem. 628 (2002) 751.
[5] S.H. Tarulli, O.V. Quinzani, E.J. Baran, O.E. Piro, E.E. Castellano, J. Mol. Struct. 656 (2003) 161.
[6] S.H. Tarulli, O.V. Quinzani, O.E. Piro, E.E. Castellano, E.J. Baran, Z. Anorg. Allg. Chem. 2003 (1975) 629.
[7] M. Dennehy, G.P. Telleria, S.H. Turulli, O.V. Quinzani, S.D. Mandolesi, J.A. Guida, G.A. Echeverria, O.E. Piro, E.C. Castellano, Inorg. Chim. Acta 360 (2007) 3169.
[8] M. Dennehy, R.M. Ferullo, O.V. Quinzani, S.D. Mandolesi, N. Castellani, M. Jennings, Polyhedron 27 (2008) 2243.
[9] M. Dennehy, G.P. Telleria, O.V. Quinzani, G.A. Echeverria, O.E. Piro, E.C. Castellano, Inorg. Chim. Acta 362 (2009) 2900.
[10] M. Dennehy, O.V. Quinzani, A. Grandos, A.R. Burrow, Polyhedron 29 (2010) 1344.
[11] S.H. Tarulli, O.V. Quinzani, O.E. Piro, E.J. Baran, E.E. Castellano, Monatsh. Chem. 132 (2001) 779.
[12] M. Vieites, D. Gambino, M. Gonzalez, H. Cerecetto, S.H. Tarulli, O.V. Quinzani, E.J. Baran, J. Coord. Chem. 59 (2006) 101.
[13] S.H. Tarulli, O.V. Quinzani, S.D. Mandolesi, J.A. Guida, G.V. Echeverria, O.E. Piro, E.E. Castellano, Z. Anorg, Allg. Chem. 645 (2009) 1604.
[14] M. Dennehy, O.V. Quinzani, S.D. Mandolesi, R.A. Burrow, J. Mol. Struct. 998 (2011) 119.
[15] S.A. Al-Jibori, I.A. Al-Nassiri, L.J. Al-Hayaly, T.A.K. Al-Allaf, Transition Met. Chem. 27 (2002) 191.
[16] O.H. Amin, L.J. Al-Hayaly, S.A. Al-Jibori, T.A.K. Al-Allaf, Polyhedron 2004 (2013) 23.
[17] S.A. Al-Jibori, A.S.S. Al-Zaubi, M.Y. Mohammed, T.A.K. Al-Allaf, Transition Met. Chem. 32 (2007) 281.
[18] S.A. Al-Jibori, A.I. Abdullah, T.A.K. Al-Allaf, Transition Met. Chem. 19 (2007) 1334.
[19] S.A. Al-Jibori, A I.A. Al-Nassiry, G. Hogarth, L. Salassa, Inorg. Chim. Acta 398 (2013) 46.
[20] S.A. Al-Jibori, T.F. Khaleel, S.A.O. Ahmed, L.J. Al-Hayaly, K. Merzweiler, C. Wagner, G. Hogarth, Polyhedron 41 (2012) 20.
[21] J.R. Meadow, J.C. Cavaguol, J. Org. Chem. 16 (1951) 1582.
[22] J.H. Price, A.N. Williamson, R.F. Schamm, B.B. Wagland, Inorg. Chem. 11 (1972) 1280.
[23] B.T. Sterenberg, H.A. Jenkins, R.J. Puddephatt, Organometallics 18 (1999) 219.
[24] SMART and SAINT+ software for CCDC diffractometers, version 6.1, Bruker AXS, Madison, WI, 2000.
[25] G.M. Sheldrick, SHELXTL PLUS, version 6.1, Bruker AXS, Madison, WI, 2000.
[26] S.A. Al-Jibori, E.G.H. Al-Saraj, N. Hollingsworth, G. Hogarth, Polyhedron 44 (2012) 210.
[27] F.S.M. Hassan, D.M. MacEwan, P.G. Pringle, B.L. Shaw, J. Chem. Soc., Dalton Trans. (1985) 1501.
[28] R.J. Puddephatt, Chem. Soc. Rev. (1983) 99.